Supplementary Information

Confining MoS_2 Nanodots into Compact Layered Graphene Blocks for High Volumetric Capacity, Fast, and Stable Sodium Storage

Shichuan Liang,[a] Su Zhang,[b] Zheng Liu,[b] Jing Feng,[a] Yuting Jiang,[a] Mingming Gao,[a] Di Geng,[a] Tong Wei,*[a, b] and Zhuangjun Fan,*[a, b]*

[a]Key Laboratory of Superlight Materials and Surface Technology, Ministry of Education; College of Materials Science and Chemical Engineering, Harbin Engineering University, Harbin 150001, P. R. China

[b]State Key Laboratory of Heavy Oil Processing, School of Materials Science and Engineering, China University of Petroleum, Qingdao 266580, P. R. China.

** Corresponding author: fanzhj666@163.com (Z. Fan); suzhangs@163.com (S. Zhang); weitong666@163.com (T. Wei)*

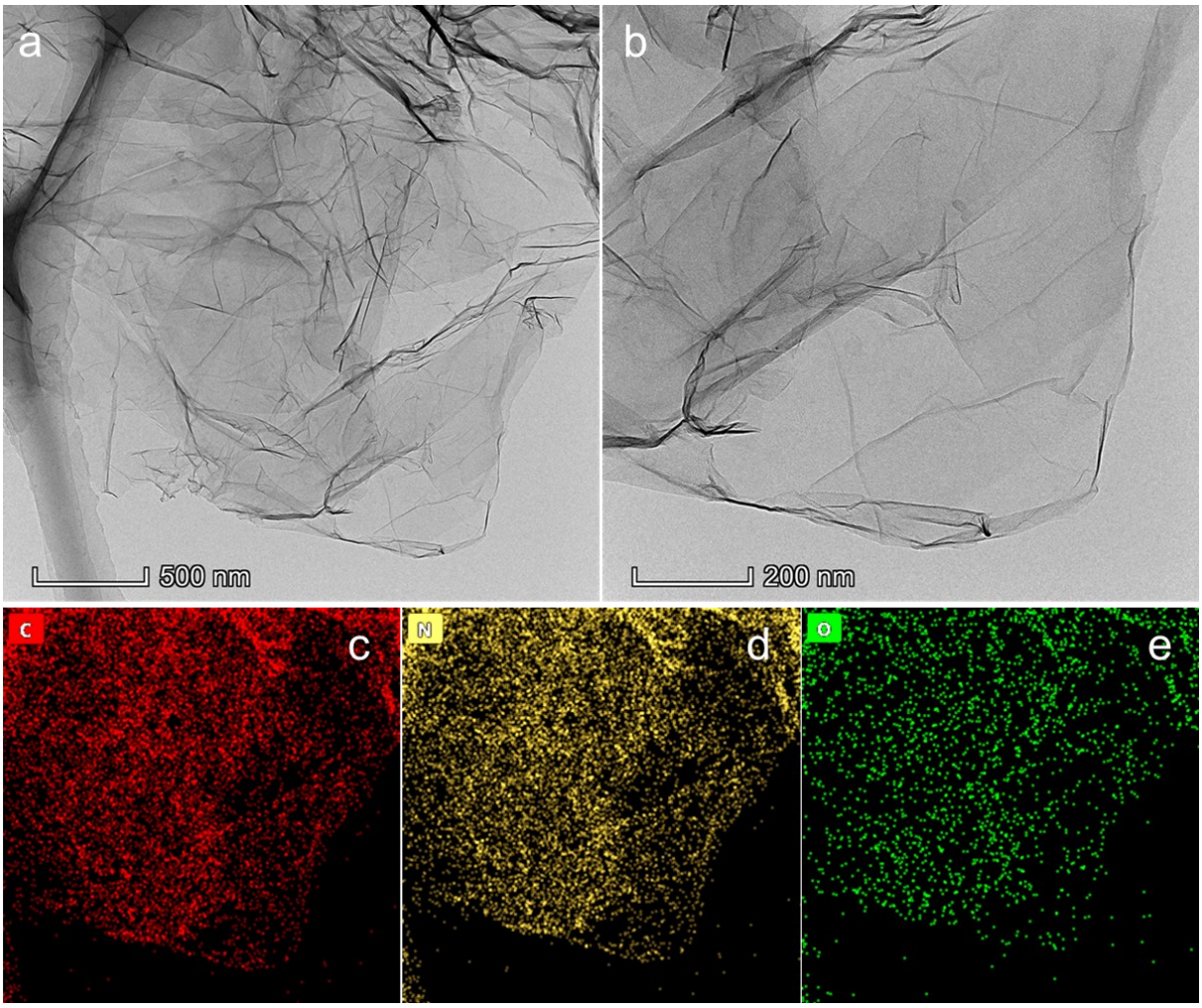

Fig. S1. (a, b) TEM images of PANI@GO, and the corresponding element mappings of (c) carbon, (d) nitrogen, and (e) oxygen elements.

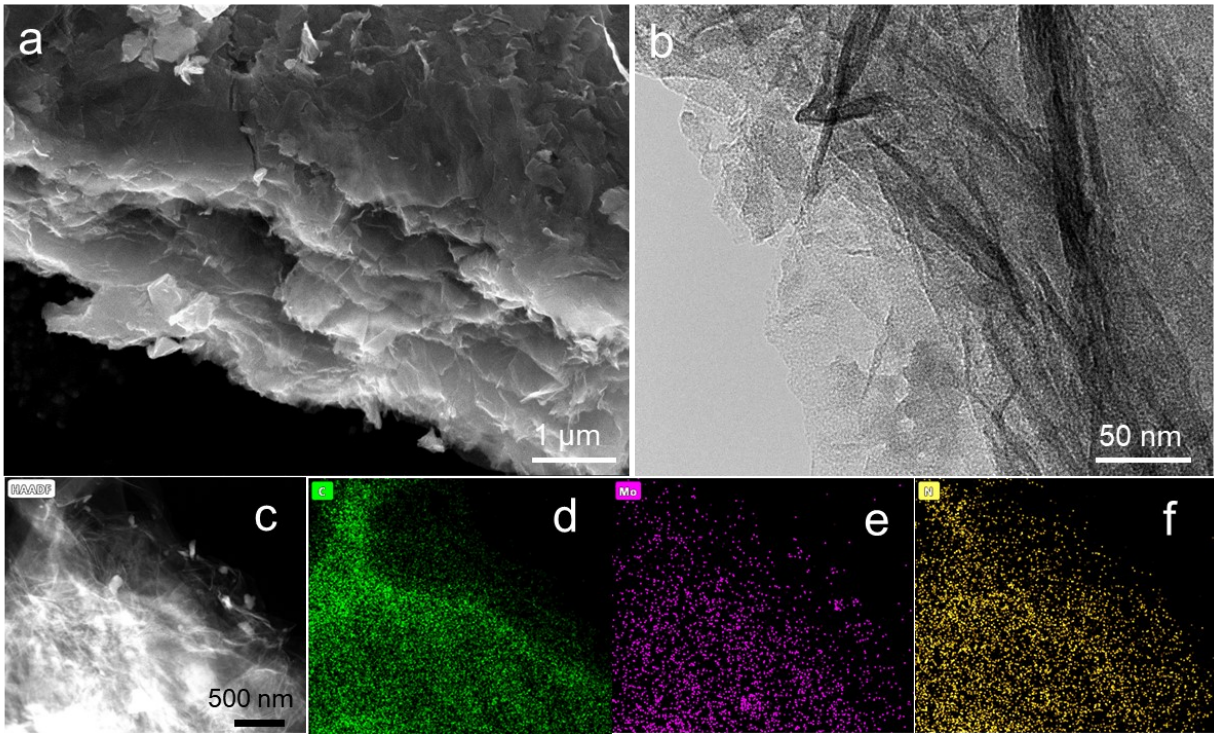

Fig. S2. (a) SEM image, (b) TEM image, (c) high-angle annular dark-field image, and the corresponding element mappings of (d) C, (e) Mo, and (f) N elements for DNG/MoS_2.

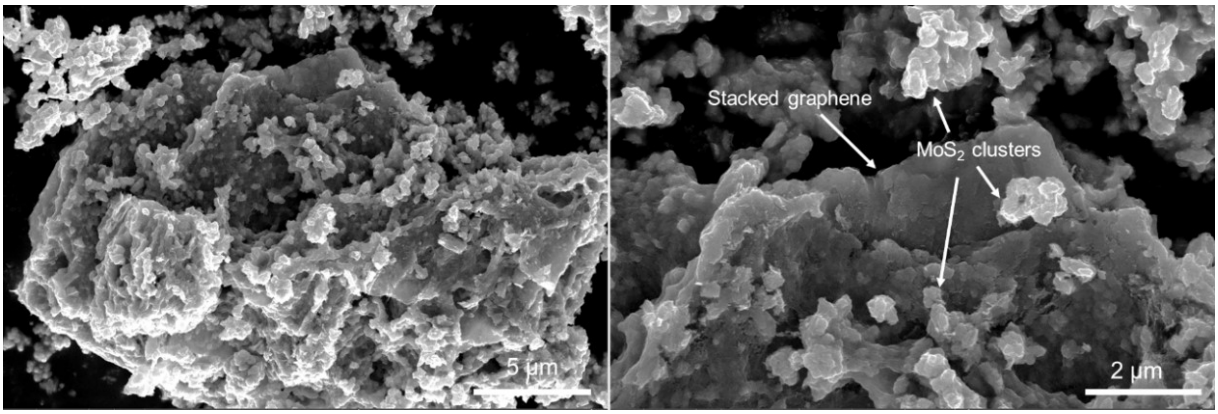

Fig. S3. SEM images of G/MoS_2.

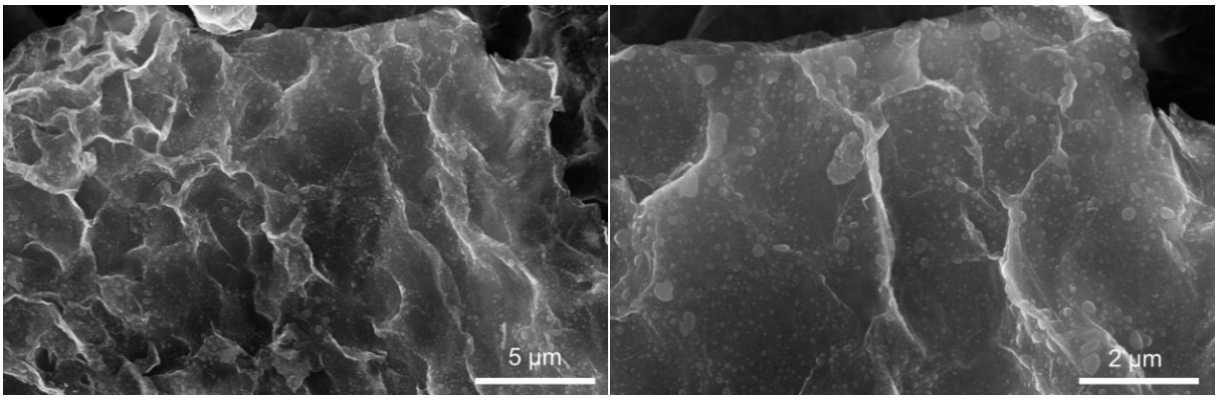

Fig. S4. SEM images of NG/MoS_2.

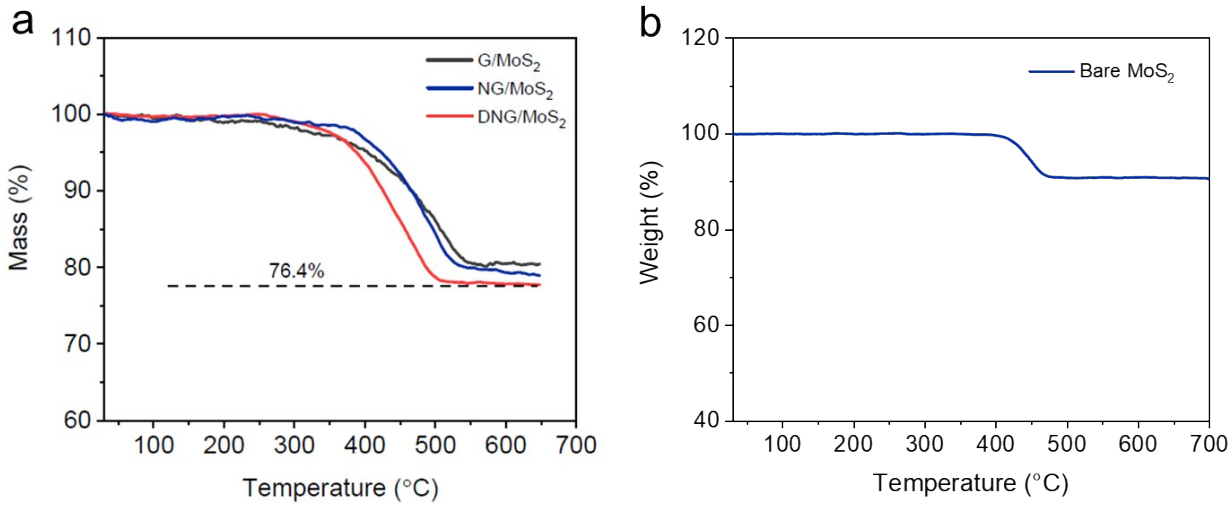

Fig. S5. (a) Thermogravimetric analysis of DNG/MoS_2, NG/MoS_2, and G/MoS_2, showing the remained weight percentage of 76.4%, 77.9%, and 79.8%, respectively. (b) Thermogravimetric analysis of bare MoS_2, showing the oxidation temperature of 400°C. For the detailed calculation of weight percentage of MoS_2 in DNG/MoS_2, G/MoS_2, and NG/MoS_2, set the initial DNG/MoS_2 mass is m, the MoS_2 weight percentage is x. Thus, the molar content of MoS_2 is $mx/160$. According to the TG curves, the remained mass percentage of MoO_3 is 76.4%, the molar content of MoO3 is 76.4%*m/144. Since the Mo atom doesn't disappear during the transformation from MoS_2 to MoO_3, leading to the equal of molar quantity between MoS_2 and MoO_3, i.e., $\frac{mx}{160} = \frac{76.4\% \times m}{144}$. Therefore, the weight percentage of MoS_2 in DNG/MoS_2 is calculated to be 84.9%. Similarly, the mass content of MoS_2 in G/MoS_2 and NG/MoS_2 are calculated to be 86.5% and 88.7%, respectively.

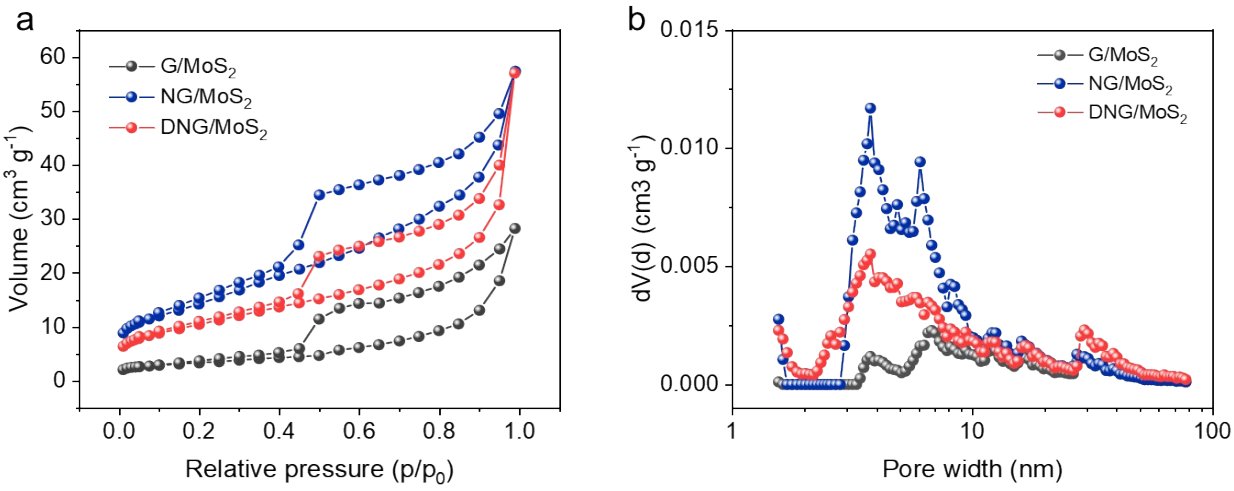

Fig. S6. N_2 adsorption-desorption isotherms for (a) G/MoS_2 and (b) NG/MoS_2.

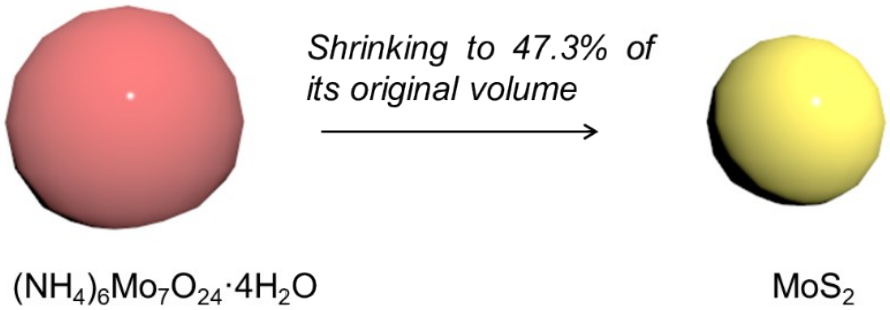

Fig. S7. Schematical illustration of volume shrinkage of $(NH_4)_6Mo_7O_{24}\cdot 4H_2O$ to MoS_2. $(NH_4)_6Mo_7O_{24}\cdot 4H_2O$ would shrink to 47.3% of its original volume after converted to MoS_2.

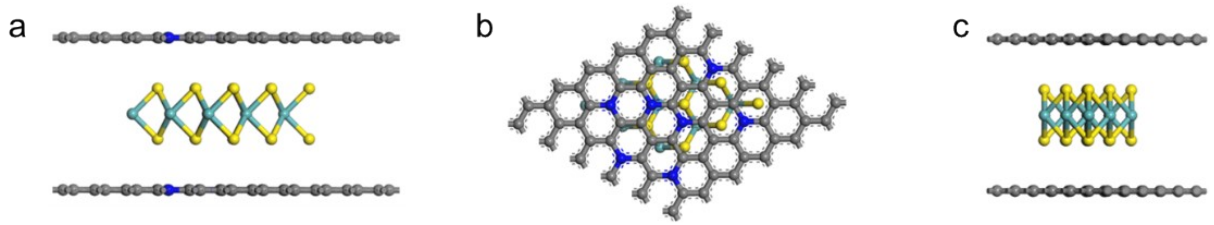

Fig. S8. The front, top, and left views of the initial DNG/MoS_2 model. The density functional theory calculations were carried out with the generalized gradient approximation (GGA) from Perdew-Burke-Ernzerhof (PBE) by using the CASTEP program of Material Studio software. The plane-wave energy cutoff was set to be 517.0 eV with a SCF tolerance of 1.0×10^{-6} eV $atom^{-1}$. The used model is based on the characteristic results of TEM image and XRD pattern, i.e., the small MoS_2 nanodots are distributed between N-doped graphene layers. The 6×6 graphene supercell and 3×3 MoS_2 supercell were used to construct DNG/MoS_2 model. The nitrogen doping type was set as graphitic N. The vacuum distance of graphene was set as 20 Å to avoid the interlayer interaction.

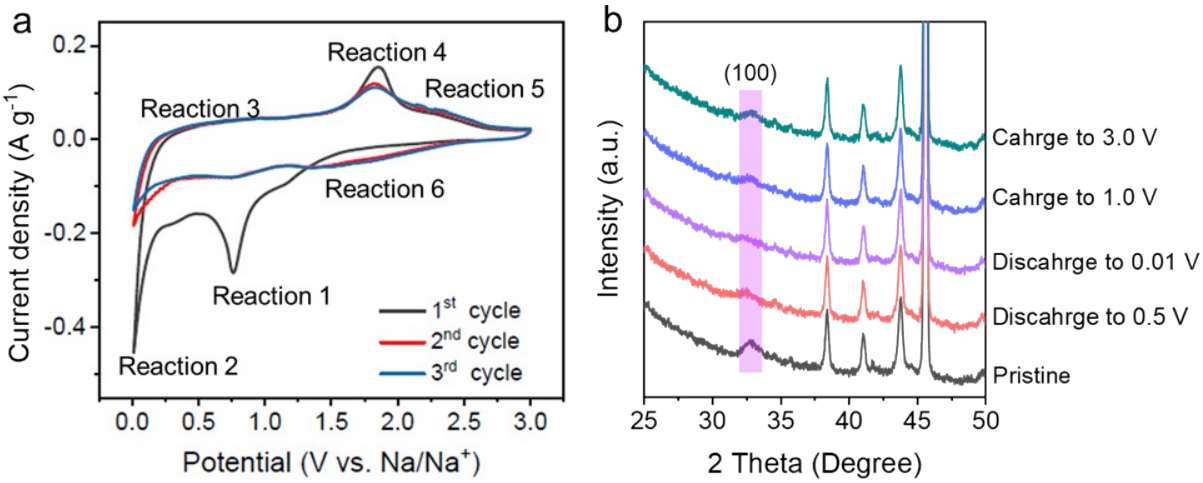

Fig. S9. (a) CV curves of DNG/MoS_2 at 0.1 mV s^{-1}. (b) In-situ XRD patterns of DNG/MoS_2 for the first cycle (the sharp peak is correlated to Be in the in-situ XRD equipment).Meanwhile, there is also the accompanying formation of S species because of the insufficient conversion (reaction 5). Thereafter, a peak at 1.8 V in second discharge cycle is correlated to the conversion of S to Na_2S (reaction 6), which is similar to the mechanism of Na/S batteries.[1, 2]

Reaction 1 (interaction, the first discharge):

$$2H - MoS_2 + xNa^+ + xe^+ \rightarrow 1T - Na_xMoS_2$$

Reaction 2 (conversion, the first discharge):

$$1T - Na_xMoS_2 + (4 - x)Na^+ + (4 - x)e^- \rightarrow 2Na_2S + Mo$$

Reaction 3 (deconversion, the first charge):

$$2Na_2S + Mo \rightarrow 1T - NaMoS_2 + 3Na^+ + 3e^-$$

Reaction 4 (deintercalation, the first charge):

$$1T - NaMoS_2 \rightarrow 1T - MoS_2 + Na^+ + e^-$$

Reaction 5 (deintercalation, the first charge):

$$Na2S + 2e^- \rightarrow 2Na + S$$

Reaction 6 (deintercalation, the second discharge):

$$S + 2Na^+ + 2e^- \rightarrow Na2S$$

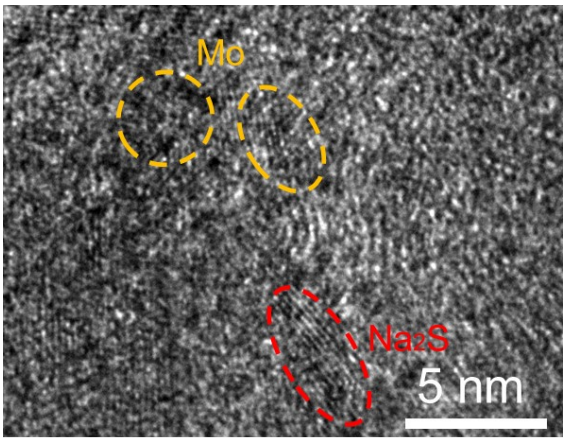

Fig. S10. High-resolution TEM image of DNG/MoS_2 electrode discharged to 0.01 V.

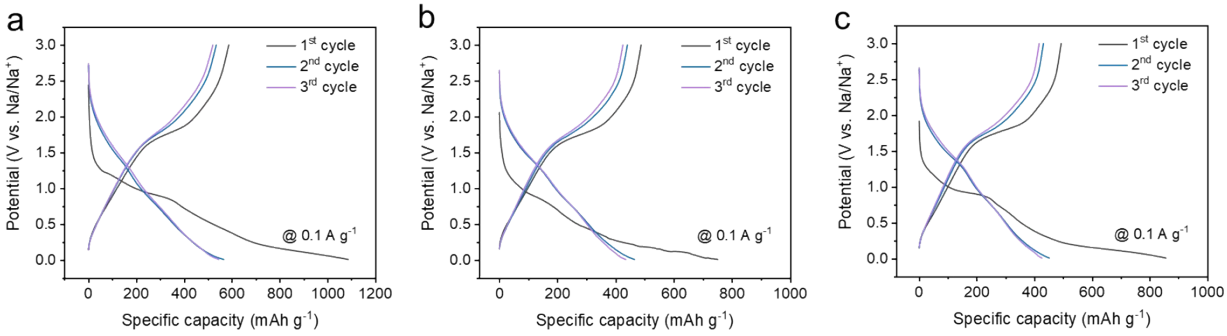

Fig. S11. The charge-discharge curves of DNG/MoS_2, NG/MoS_2, and G/MoS_2 at 0.1 A g^{-1} for the first three cycles.

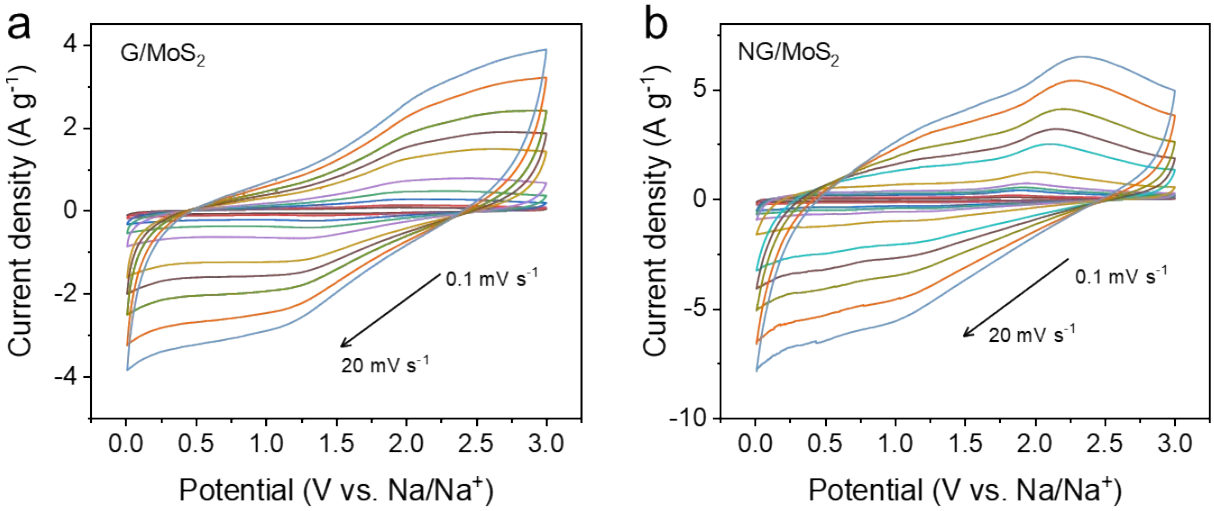

Fig. S12. CV curves at the scan rates from 0.1 to 20 mV s^{-1} for (a) G/MoS_2 and (b) NG/MoS_2.

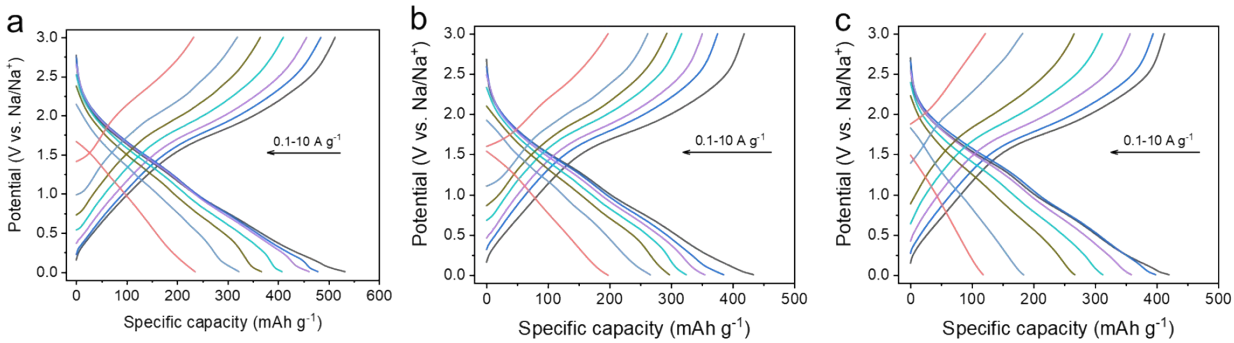

Fig. S13. The charge-discharge curves of DNG/MoS_2, NG/MoS_2, and G/MoS_2 at different current densities from 0.1 to 10 A g^{-1}.

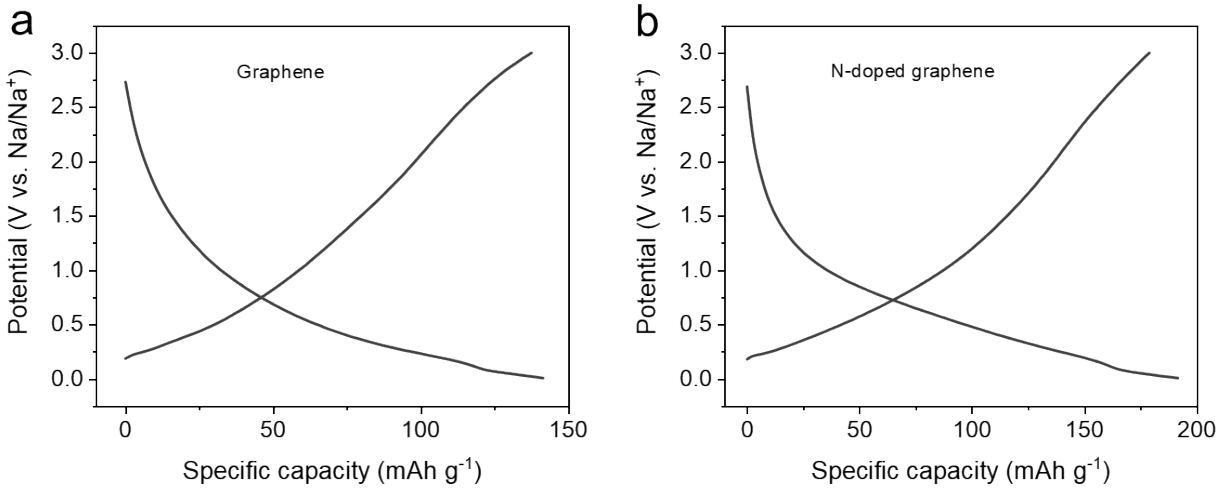

Fig. S14. Discharge-charge profiles of graphene and N-doped graphene at 0.1 A g^{-1}. The galvanostatic charge-discharge profiles show the discharge capacities of 192 mAh g^{-1} and 141 mAh g^{-1} at 0.1 A g^{-1} for N-doped graphene and graphene nanosheets, respectively. Taking DNG/MoS_2 as an example, the mass content of MoS_2 is determined to be 84.9 wt.%, i.e., there is 15.1 wt.% of N-doped graphene in DNG/MoS_2. Based on the equation:

$$C_{NG\ in\ DNG/MoS_2} = C_{NG} \times M_{NG}$$

where the C_{NG} and M_{NG} are capacities delivered by N-doped graphene and mass content of N-doped graphene, respectively. $C_{NG\ in\ DNG/MoS2}$, the capacity contribution of N-doped graphene in DNG/MoS_2, is calculated to be 29 mAh g^{-1}, which accounts for only 5.6% of DNG/MoS_2 (514 mAh g^{-1} at 0.1 A g^{-1}). The graphene and N-doped graphene contents in G/MoS_2 and NG/MoS_2 are 11.3% and 13.5%, respectively. By the same procedure, the capacity contributions of graphene and N-doped graphene in D/MoS_2 and NG/MoS_2 are calculated to be 16 and 26 mAh g^{-1}, accounting for only 3.8% and 5.9% in G/MoS_2 and NG/MoS_2, respectively.

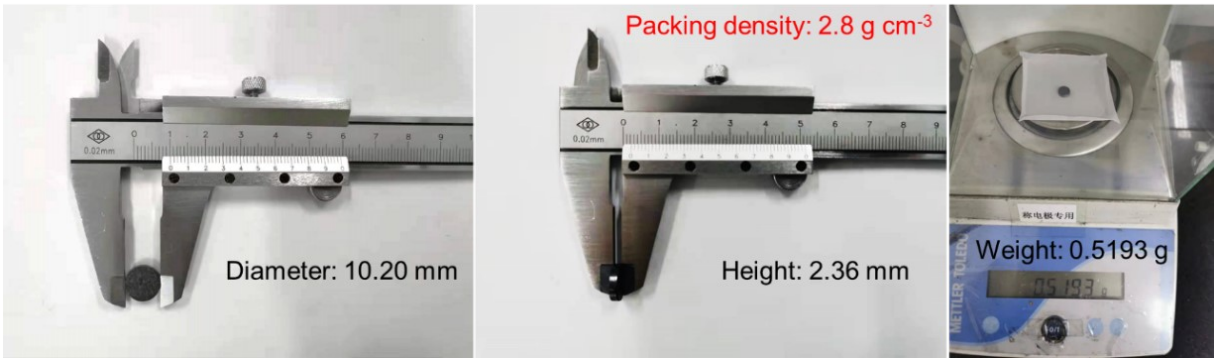

Fig. S15. The optical photographs of the compressed DNG/MoS_2 tablet. DNG/MoS_2 was compressed using a laboratorial hydraulic machine in a FT-IR die under the pressure of 10 MPa, which is equal to the pressure of electrode calendaring.

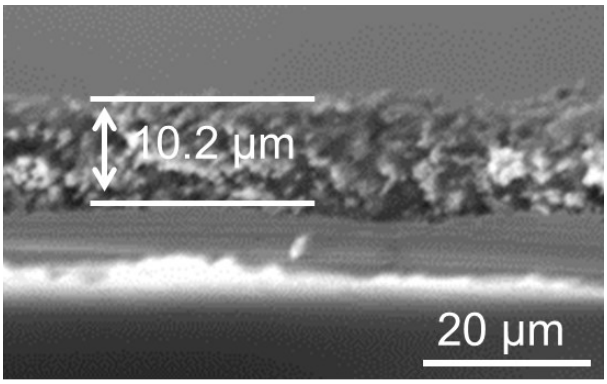

Fig. S16. SEM image of DNG/MoS_2 electrode before sodiation. To calculate the volumetric capacity of the slurry casting electrode, in detail, the thickness (*h*) of slurry casting electrode is 10.2 μm, the area (*S*) is 0.785 cm^{-2}, the volume (*V*) of slurry casting electrode is $V = \pi \times S$; the specific capacity (*Cs*) of DNG/MoS_2 at 0.1 A g^{-1} is 514 mAh g^{-1}, the mass of DNG/MoS_2 (*m*) is 1.2 mg, the capacity delivered by DNG/MoS_2 in slurry casting slurry electrode (*C*) is $C = Cs \times m$. Therefore, the volumetric capacity of slurry casting electrode (*Cv*) can be calculated by equation $Cv = \frac{C}{V}$, resulting in 770 mAh cm^{-3} at 0.1 A g^{-1}.

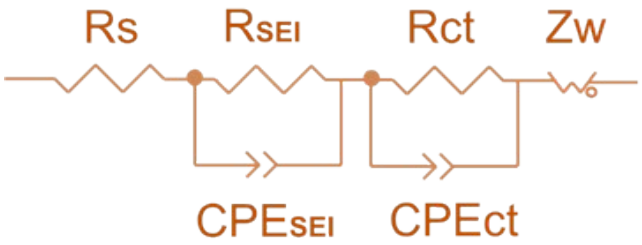

Fig. S17. Equivalent circuit for EIS spectra.

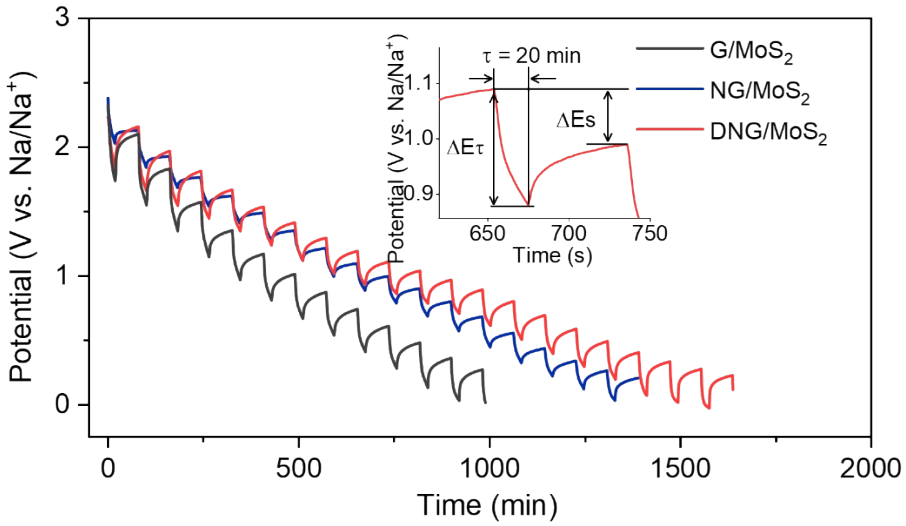

Fig. S18. Discharge GITT curves of DNG/MoS_2, NG/MoS_2, and G/MoS_2. The cell was discharged at 0.1 A g^{-1} for 20 min and then relaxed for 60 min to enable the potential equilibrium. The D_{Na} can be calculated by the simplified equation: [3]

$$D_{Na} = \frac{4}{\pi\tau}\left(\frac{m_B V_M}{M_B A}\right)^2\left(\frac{\Delta E_S}{\Delta E_\tau}\right)^2$$

where τ is the duration time of the current pulse, m_B is the mass of the active material (g), M_B is the molecular weight (g mol^{-1}), V_M is the molar volume (cm^3 mol^{-1}), A is the total contact area between electrode and electrolyte (cm^2), $\Delta E\tau$ is the change of transient voltage (V), and ΔE_S is related to the change of steady-state voltage for the corresponding step.

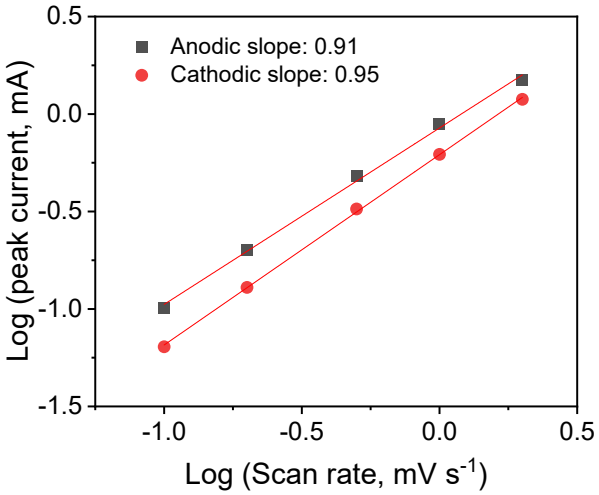

Fig. S19. Current response against the scan rates at peak potentials of DNG/MoS_2.

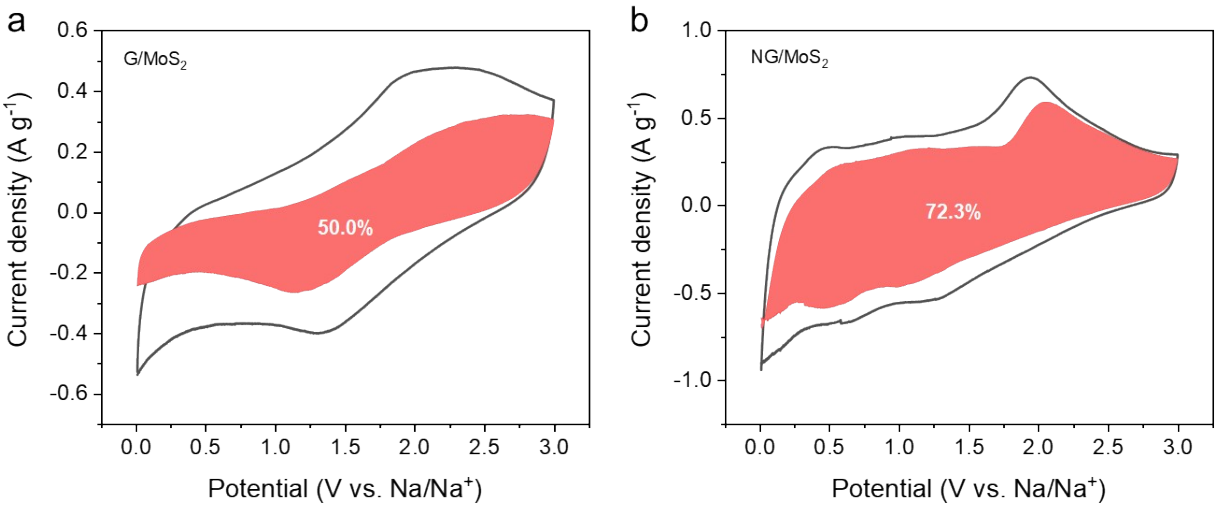

Fig. S20. Capacitive contributions of (a) G/MoS_2 and (b) NG/MoS_2 at 1 mV s^{-1}. The quantitative capacitive contribution under the given scan rate is obtained based on the following equation:[4]

$$i = k_1 v + k_2 v^{1/2}$$

$$i/v^{1/2} = k_1 v^{1/2} + k_2$$

where k_1 and k_2 are appropriate values, i (A g^{-1}) is current density, v (mV s^{-1}) is scan rate, and $k_1 v$ and $k_2 v^{1/2}$ are capacitive contribution and diffusion contribution, respectively.

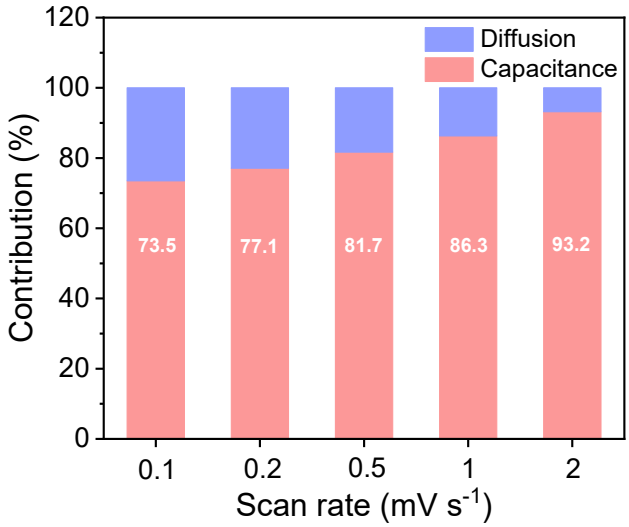

Fig. S21. Capacitance contributions for DNG/MoS_2 at different scan rates.

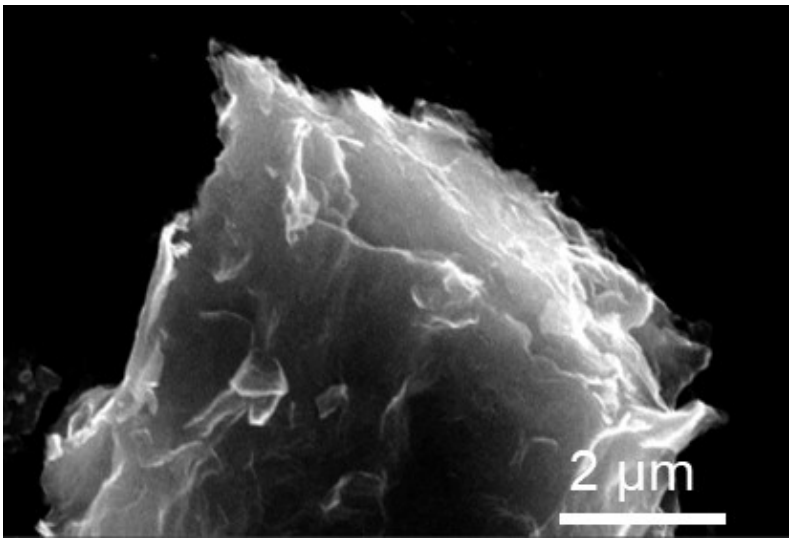

Fig. S22. SEM image of post-cycled DNG/MoS_2 electrode.

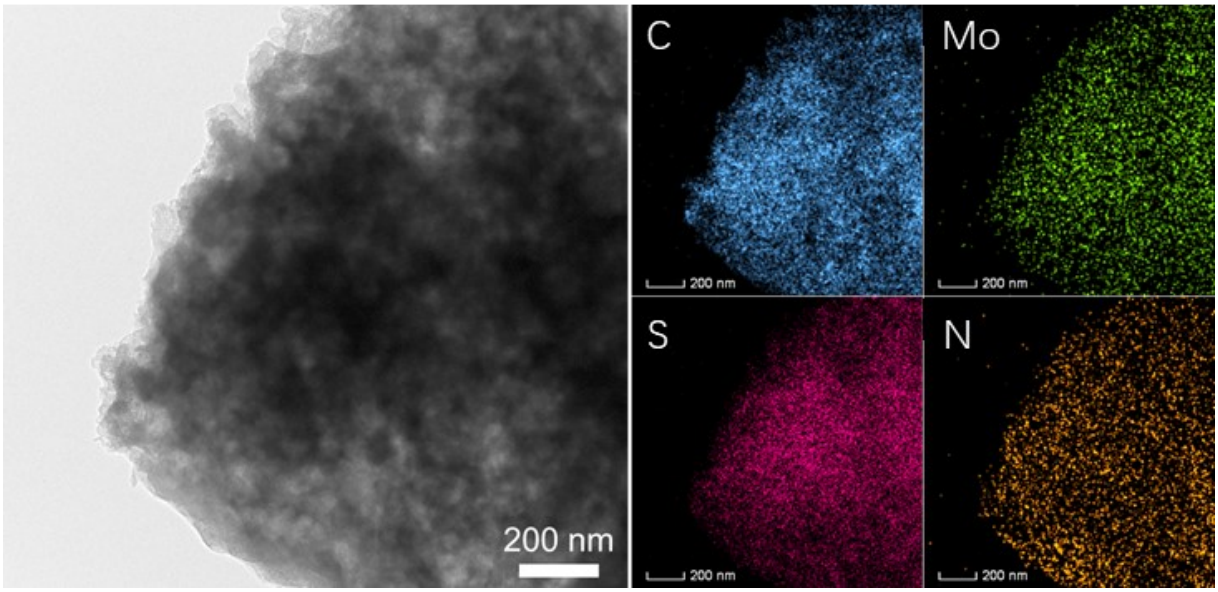

Fig. S23. TEM image and the corresponding element mappings of the post-cycled DNG/MoS_2.

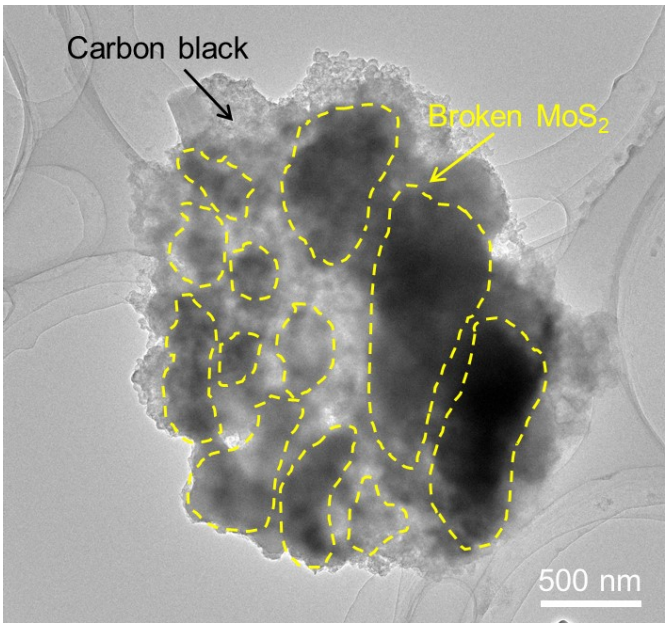

Fig. S24. TEM image of the post-cycled bare MoS_2 electrode.

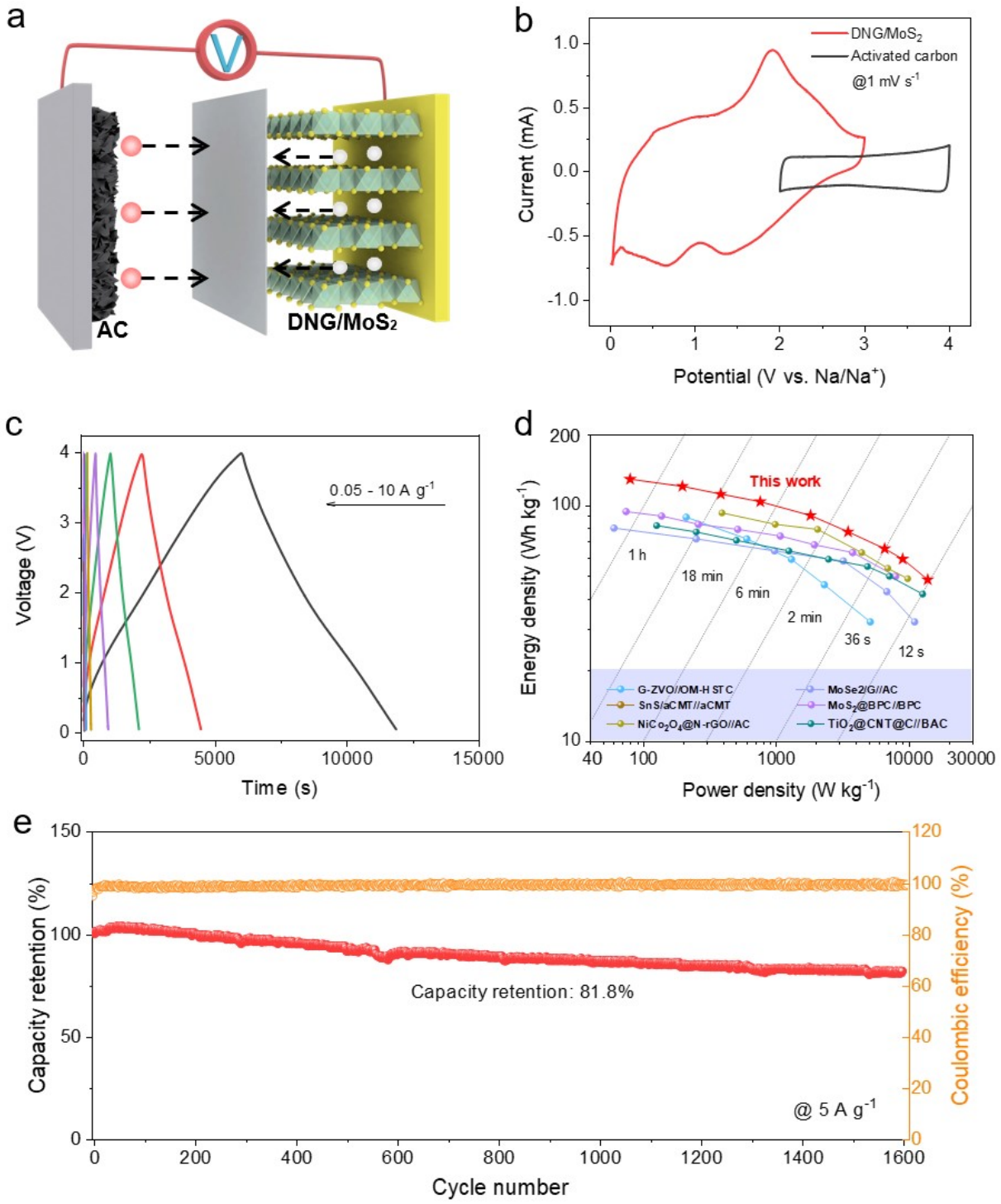

Fig. S25. (a) Schematic illustration of assembled activated carbon//DNG/MoS_2 SIC. (b) CV curves of activated carbon and DNG/MoS_2 at scan rate of 1 mV s^{-1}. (c) Galvanostatic charge-discharge profiles of the SIC at current densities of 0.1-50 A g^{-1}. (d) Comparison of Ragone plots of the activated carbon//DNG/MoS_2 SIC with previously reported SICs. (e) Cycle performance of as-assembled SIC at 5 A g^{-1}.

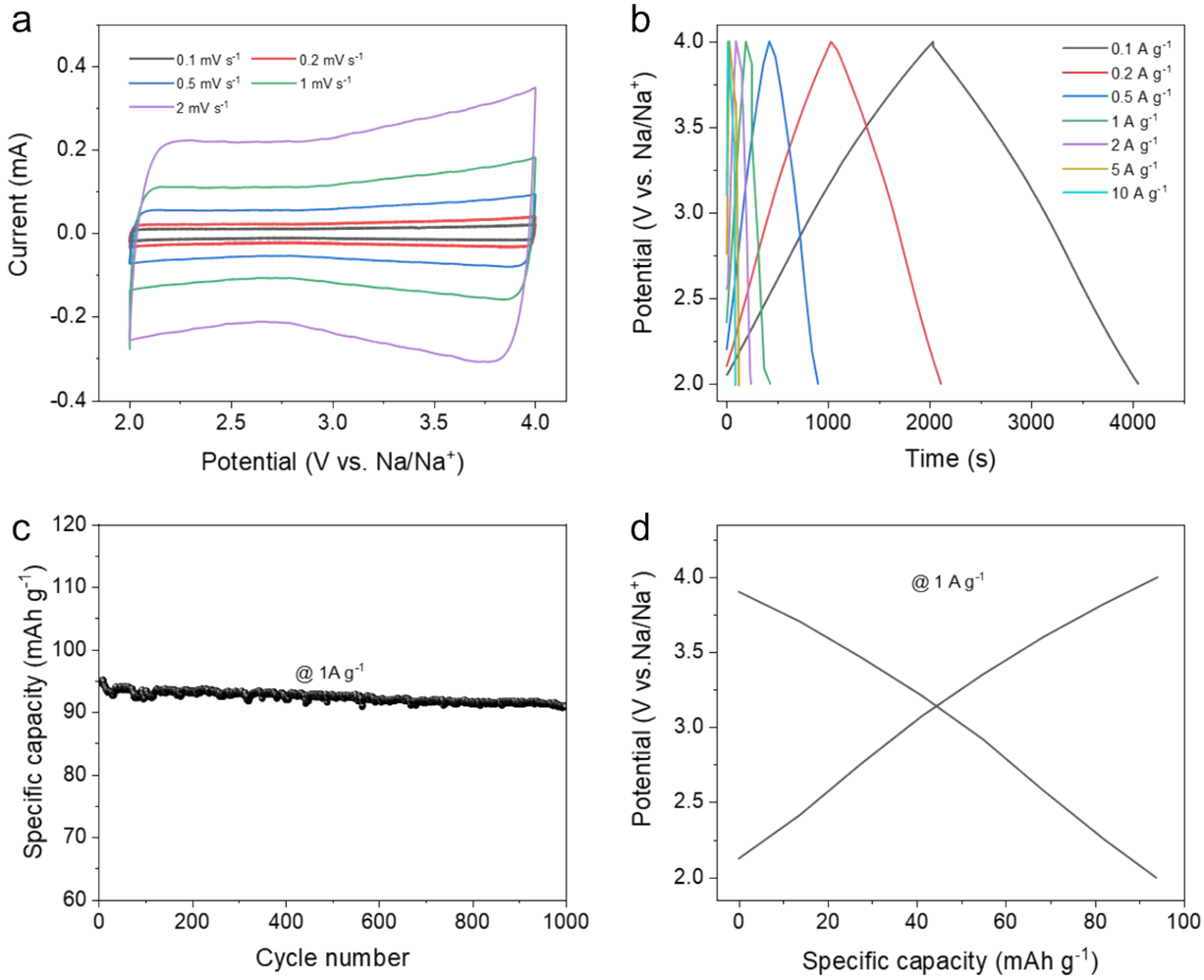

Fig. S26. The electrochemical performance of activated carbon at the potential window of 2-4 V in sodium half-cell: (a) CV curves at scan rates from 0.1 to 2 mV s^{-1}, (b) discharge-charge profiles from 0.1 to 10 A g^{-1}, (c) cycling performance at 1 A g^{-1}, and (d) discharge-charge profiles at 1 A g^{-1}.

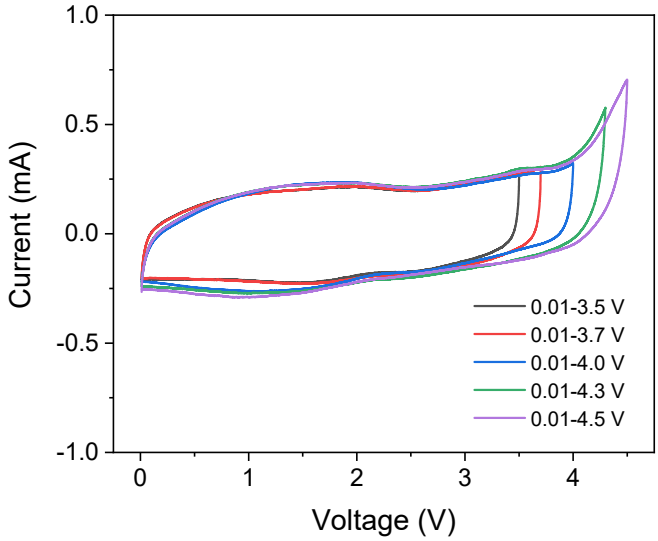

Fig. S27. CV curves of DNG/MoS_2//activated carbon SIC with a minimum voltage of 0.01 V and various maximum voltage of 3.5-4.5 V at 1 mV s^{-1}.

Table S1. The pore volumes and the specific surface areas of DNG/MoS_2, NG/MoS_2, G/MoS_2, and D-Mo/PANI@GO.

Samples	Pore volume (cm^{-3} g^{-1})	Specific surface area (m^2 g^{-1})
DNG/MoS_2	0.086	37.3
NG/MoS_2	0.086	54.3
G/MoS_2	0.041	10.4
D-Mo/PANI@GO	---	8.6

Table S2. The electronical conductivity of bare MoS_2 and DNG/MoS_2.

Samples	Electronical conductivity (S cm^{-1})			Average value (S cm^{-1})
Bare MoS_2	$24.5*10^{-6}$	$28.4*10^{-6}$	$35.8*10^{-6}$	$29.6*10^{-6}$
DNG/MoS_2	11.0	10.3	9.8	10.4

Table S3. The resistance values of DNG/MoS_2, NG/MoS_2, and G/MoS_2.

Samples	Rs (Ω)	R_{ct} (Ω)	Z_w (Ω)
G/MoS_2	3.8	243.9	595.0
NG/MoS_2	2.8	453.8	403.5
DNG/MoS_2	2.2	86.2	194.2

Calculations

Electrochemical calculations for the assembled sodium ion capacitor

The specific capacitance (F g^{-1}) of sodium ion capacitor is calculated by the following equation:

$$C = \frac{I\Delta t}{\Delta V}$$

where I (A g^{-1}) is the current density, Δt (s) is the discharge time, and ΔV (V) is the voltage window.

The specific energy density (E, Wh kg^{-1}) and specific power density (P, W kg^{-1}) were calculated by the following equation:

$$E = \frac{1}{2}CV^2$$

$$P = \frac{E}{\Delta t}$$

where C (F g^{-1}) is the specific capacitance, V is the voltage range of discharge process excluding the IR drop, and Δt (s) is the discharge time. Here, the energy density (Wh kg^{-1}) and power density (W kg^{-1}) of the SICs were calculated based on the total mass of cathode and anode.

Reference

1. B. Chen, T. Wang, S. Zhao, J. Tan, N. Zhao, S. P. Jiang, Q. Zhang, G. Zhou and H.-M. Cheng, *Adv. Mater.,* 2021, **33**, 2007090.
2. B. Chen, H. Lu, J. Zhou, C. Ye, C. Shi, N. Zhao and S.-Z. Qiao, *Adv. Energy Mater.,* 2018, **8**, 1702909.
3. S. Li, Y. Liu, X. Zhao, Q. Shen, W. Zhao, Q. Tan, N. Zhang, P. Li, L. Jiao and X. Qu, 2021, *Adv. Mater.,* 2021, **33**, 2007480.
4. C. Zhao, C. Yu, M. Zhang, Q. Sun, S. Li, M. Norouzi Banis, X. Han, Q. Dong, J. Yang, G. Wang, X. Sun and J. Qiu, *Nano Energy*, 2017, **41**, 66-74.